Preprints, Fourth IFAC Conference on
Modelling, Identification and Control of Nonlinear Systems
Lyon, France. September 4-6, 2024

Ethanol regulation in yeast fed-batch cultures by stabilizing extremum seeking

Laurent Dewasme * **Alain Vande Wouwer** *

* *Systems, Estimation, Control and Optimization (SECO) , University of Mons, 7000 Mons, Belgium (e-mail: <laurent.dewasme, alain.vandewouwer>@umons.ac.be).*

Abstract: In this study, an original model-free stabilizing extremum seeking (STAB-ESC) strategy is applied to optimize yeast fed-batch culture productivity. To this end, the ethanol concentration is tracked at a low level, to approach the yeast growth optimal conditions. Overflow metabolism effects, resulting from the cell's limited respiratory capacity, are considered using a macroscopic model with discontinuous kinetics. The detrimental impact of input saturation on the proposed STAB-ESC stability is overcome using a state-dependent switching control strategy. The resulting methodology is illustrated with numerical results where the robustness of the controller to measurement noise is also highlighted.

Keywords: Data-driven control, stabilization, extremum seeking, averaging, switching system.

1. INTRODUCTION

Industrial vaccine production depends on essential steps including the upstream and downstream processes. Recombinant protein production in bioreactors is the most critical step of the upstream chain (Silva et al., 2022), where genetically modified host strains are cultivated. The fed-batch mode, where the bioreactor is gradually filled without medium withdrawal, is popular because of its simplicity and good performance. A diversity of host strains can be exploited, including yeast, bacteria, and mammalian cells, and in the sequel of this study, attention will be focused on fed-batch cultures of yeast strains.

Even if fed-batch cultures can reach high biomass densities, the metabolic switches that yeast encounter, depending on the quantity of substrate, make the tracking of good operating conditions a difficult task since it impacts the process productivity (i.e., the quantity of product of interest over time). Yeasts are indeed likely to follow two main metabolic pathways, exhibiting overflow metabolism (or short-term Crabtree effect, Crabtree (1929)) when the substrate is fed in excess or starving metabolism in the opposite case. Overflow metabolism leads to the accumulation of ethanol by fermentation, which tends to inhibit the yeast's oxygen capacity and, in turn, the biomass growth.

An optimal feeding strategy must therefore be established, ideally tracking the critical substrate level representing the boundary between both overflow and starving pathways (Dewasme et al., 2011b; Akesson et al., 1999). However, this critical level corresponds to a substrate concentration's order of magnitude which is often below the sensitivity level of existing probes, and remains undetectable. Therefore, a sub-optimal but still efficient solution, considering the regulation of the metabolic by-product as low as the probe allows it, can be adopted. Several strategies have been proposed under this principle (Valentinotti et al., 2003; Renard et al., 2006; Dewasme et al., 2010; Pimentel et al., 2015; Ibanez et al., 2021) which usually rely on adaptive and/or robust control formulations and require a trustful online estimation of the biomass growth-related parameters and variables.

In the study of Dewasme et al. (2011a), the robustness limits of adaptive linearizing control are highlighted, correlating the performance degradation with an increasing measurement variance. The development of reliable and robust adaptive controllers is still an open topic and among the several possible solutions, extremum-seeking (ES) algorithms have received renewed attention during the last two decades (Ariyur and Krstic, 2003; Tan et al., 2010; Scheinker, 2024). ES is a direct output adaptation scheme that allows finding the optimum of a steady-state cost function, assumed to be measurable. Many properties of ES have been studied, highlighting considerable accuracy and convergence improvements (Moase and Manzie, 2012; Guay and Dochain, 2017; Poveda and Krstic, 2021). The resulting strategies have been intensively exploited in several fields (Ghaffari et al., 2014; Chichka et al., 2006; Koeln and Alleyne, 2014), and, more recently, also in biotechnological process optimization (Dewasme and Vande Wouwer, 2020; Feudjio Letchindjio et al., 2021).

Studies connecting ESC to Lyapunov functions (Sontag, 1989) show particularly promising performance characterized by (i) a high-gain estimation (in contrast with the classical ES theory based on modulation-demodulation filtering) and (ii) a robust-to-noise behavior. The latter is due to the guaranteed bounds on the input update conferred by the inclusion of the measured cost function in the periodic dither signal (Scheinker and Krstić, 2017). The resulting algorithm is called Stabilizing ES (STAB-ES) with convergence properties founded on Lie-bracket averaging theory (Dürr et al., 2013).

Most of the ES strategies dedicated to fed-batch applications often rely on a model to track the optimal exponential feeding trajectory (Titica et al., 2003; Marcos et al., 2004). A model-free alternative is however proposed by Dewasme et al. (2011b), but at the cost of a complex probing configuration. The motivation of the present study is to investigate the inclusion of STAB-ES in a simple model-free adaptive control scheme regulating

the ethanol concentration of yeast fed-batch cultures. Some stability and robustness analyses are provided in the presence of detrimental effects such as input saturation and measurement noise.

This paper is organized as follows: section 2 briefly presents the considered yeast growth model. Section 3 discusses the control strategy including a review of the STAB-ESC stability results and design guidelines while section 4 provides a detailed analysis of the numerical simulations. Conclusions are drawn in section 5.

2. BIOPROCESS DESCRIPTION

We first consider the mechanistic model of (Dewasme et al., 2011b) describing the *Saccharomyces cerevisiae* yeast strain catabolism through three main pathways:

$$\text{Glucose oxidation} : \mathrm{G} \overset{r_1 X}{\rightarrow} k_{X1}\,\mathrm{X} \tag{1a}$$

$$\text{Glucose fermentation} : \mathrm{G} \overset{r_2 X}{\rightarrow} k_{X2}\,\mathrm{X} + k_{E2}\,\mathrm{E} \tag{1b}$$

$$\text{Ethanol oxidation} : \mathrm{E} \overset{r_3 X}{\rightarrow} k_{X3}\,\mathrm{X} \tag{1c}$$

where X, G, and E are, respectively, the concentrations in the culture medium of biomass, glucose and ethanol. $k_{\xi i}$ ($\xi = X, G, E$, and $i = 1,2,3$) are the yield coefficients and r_1, r_2 and r_3 are the nonlinear specific growth rates given by:

$$r_1 = \min\left(r_G, r_{G_{crit}}\right) \tag{2}$$

$$r_2 = \max\left(0, r_G - r_{G_{crit}}\right) \tag{3}$$

$$r_3 = \max\left(0, \frac{r_{G_{crit}} - k_{os} r_G}{k_{oe}} \frac{E}{K_E + E}\right) \tag{4}$$

where k_{os} and k_{oe} are the oxidative yield coefficients respectively related to the substrate and ethanol oxidations. The kinetic terms associated with the glucose consumption r_G and the critical glucose consumption $r_{G_{crit}}$ (function of the cell respiratory capacity r_O) are given by:

$$r_G = \mu_G \frac{\mathrm{G}}{\mathrm{G} + K_G} \tag{5a}$$

$$r_{G_{crit}} = \frac{r_O}{k_{os}} = \frac{\mu_O}{k_{os}} \frac{Ki_E}{Ki_E + E} \tag{5b}$$

These expressions take the classical form of Monod laws (Monod, 1949) where μ_G and μ_O are the maximal values of specific growth rates, K_G, and K_E are the saturation constants of the corresponding element, and Ki_E is the inhibition constant.
This kinetic model is based on Sonnleitner's bottleneck assumption (Sonnleitner and Käppeli, 1986). The cells are likely to change their metabolism because of their limited oxidative capacity. When glucose is in excess ($G > G_{crit}$, and $r_G > r_{G_{crit}}$), the metabolism follows the fermentation (or overflow) pathway. On the other hand, when glucose becomes limiting ($G < G_{crit}$ and $r_G < r_{G_{crit}}$), its available quantity is oxidized, and the remaining respiratory capacity is used to oxidize ethanol as the cells switch to a starving metabolism.

Component-wise mass balance gives the following differential equations:

$$\frac{dX}{dt} = (k_{X1} r_1 + k_{X2} r_2 + k_{X3} r_3) X - DX \tag{6a}$$

$$\frac{dG}{dt} = -(r_1 + r_2) X + D G_{in} - DG \tag{6b}$$

$$\frac{dE}{dt} = (k_{E2} r_2 - r_3) X - DE \tag{6c}$$

$$\frac{dV}{dt} = F_{in} \tag{6d}$$

where G_{in} is the glucose concentration in the feed, F_{in} is the inlet feed rate, V is the culture medium volume and D is the dilution rate ($D = F_{in}/V$). All stoichiometric and kinetic parameter values are respectively reported in Tables 1 and 2.

Table 1. Yield coefficients values of Sonnleitner and Käppeli *S. cerevisiae* model

Yield coefficients	Values	Units
k_{X1}	0,49	g of X/g of S
k_{X2}	0,05	g of X/g of S
k_{X3}	0,72	g of X/g of E
k_{E2}	0,48	g of E/g of S
k_{os}	0,3968	g of O_2/g of S
k_{oe}	1,104	g of O_2/g of E

Table 2. Kinetic coefficients values of Sonnleitner and Käppeli *S. cerevisiae* model

Kinetic coefficients	Values	Units
μ_O	0,256	g of O_2/g of X /h
μ_S	3,5	g of S/g of X /h
K_S	0,1	g of O_2/L
K_E	0,1	g of E/L
Ki_E	10	g of E/L

3. CONTROL STRATEGY

3.1 Ethanol regulation

The critical glucose concentration is often low (of the order $O(10^{-2})g/L$) and online hardware or even software probe sensitivities may become insufficient (Dewasme et al., 2009), delivering inaccurate measurements. Moreover, the tolerance of cells to metabolic switches is relatively limited and the critical glucose regulation strategy may be unsuitable.

Reconsidering the objective into a more practical suboptimal configuration therefore makes sense. Limiting or regulating the ethanol concentration at a level above the sensitivity of commercially available probes (typically in the range of $0.1g/l$) will offer significant productivity improvement (Dewasme et al., 2010).

It may be assumed that the suboptimal strategy operates in the neighborhood of the optimal productivity conditions leading to a low glucose concentration G which can be considered in quasi-steady. The small accumulated quantity of substrate V G is indeed almost instantaneously consumed by the cells ($\frac{dG}{dt} \approx 0$ and $G \approx 0$) and (6b) becomes:

$$r_2 X = -r_1 X + D G_{in} \tag{7}$$

Replacing $r_2 X$ by (7) in the mass balance equation of E (6c) yields:

$$\dot{E} = -k_{E2} r_1 X - r_3 X - D\left(E - k_{E2} G_{in}\right) \tag{8}$$

and the tracking error system considering a constant set-point E^* reads:

$$\frac{d(E^*-E)}{dt} = k_{E2}r_1X + r_3X + D\,(E - k_{E2}G_{in}) \tag{9}$$

3.2 Trajectory tracking by STAB-ES

We consider a generic form of the error system (9) as follows:

$$\dot{e} = f(\underline{x}) + g(\underline{x})u \tag{10}$$

where $e = E^* - E$ is the error variable, $\underline{x} \in \mathbb{R}^{+,n}$ is the state vector ($\underline{x} = [X\ G\ E]$, $n = 3$), $f, g : \mathbb{R}^{+,n} \to \mathbb{R}$ are general nonlinear functions, i.e. $f(\underline{x}) = k_{X1}r_1X + r_3X$ and $g(\underline{x}) = E - k_{E2}G_{in}$. $u \in \mathbb{R}^+$ is a scalar input (the dilution rate D).

The stabilizing extremum seeking controller for trajectory tracking is designed as follows:

$$u = \alpha\sqrt{\omega}\,cos\,(\omega\,t) - k\,\sqrt{\omega}\,sin\,(\omega\,t)\,V(\underline{x}) \tag{11}$$

where V is a Cost Lyapunov Function (CLF), ω is the pulsation (assumed to be large) of the periodic seeking signal (11), α and k are parameters which, a priori, are respectively used to tune the magnitude of (11). We propose the following CLF, assumed to be measurable:

$$V(\underline{x}) = \eta\ X\ \ |e| \tag{12}$$

where η is a positive constant, chosen such that the following upper bound of the absolute value of f holds: $|f(\underline{x})| \leq \eta\ X$. From the definition of the kinetics in (2), (3), and (4), the validation of this boundedness assumption is straightforward.

3.3 Weak limit for averaging

To study the dynamics of the stabilizing ESC, the average closed-loop trajectory is commonly computed to approximate the solution of the actual periodically disturbed system (Khalil, 2002). This approximation is represented by the average of (11) when considering a small parameter ε. This equation can be rewritten after rescaling time in $\tau = \omega t$ and setting $\varepsilon = \frac{1}{\omega}$ as in (Dürr et al., 2013):

$$\dot{\underline{x}} = f(\underline{x}) + g\,(\underline{x})\left(\frac{\alpha}{\sqrt{\varepsilon}}cos(\tau) - \frac{k}{\sqrt{\varepsilon}}sin(\tau)V(\underline{x})\right) = \mathcal{F}\,(\underline{x},\tau,\varepsilon) \tag{13}$$

Applying averaging to system (13) is therefore impossible due to the presence of the factor $\frac{1}{\sqrt{\varepsilon}}$ in $\mathcal{F}$ (averaging requires that $\mathcal{F}\,(\tau,u,0)$ exists). Therefore, a Lie bracket averaging analysis is used instead, based on the definition of a weak limit. For the sake of clarity, we review the main results of Scheinker and Krstić (2017) and, more particularly, theorem 2.3 applied to (10), which we first expand as follows, renaming each factor as h_1, b_1, h_2 and b_2:

$$\dot{e} = f(\underline{x}) + \underbrace{\alpha\,\sqrt{\omega}\,cos\,(\omega\,t)}_{h_1}\ \underbrace{g(\underline{x})}_{b_1} \underbrace{-\alpha\,\sqrt{\omega}\,sin\,(\omega\,t)}_{h_2}\ \underbrace{kg(\underline{x})V(\underline{x})}_{b_2} \tag{14}$$

The averaging step consists of finding a way to compute (14) when ω tends to infinity, using the concept of weak limits. Studying the weak limit of h_1 and h_2 requires the use of the *Riemann-Lebesgue* Lemma which states that, for a function $f(x)$ defined on a compact set C of the Lebesgue-integrable space (i.e., $L^1(C)$),

$$\lim_{\omega\to\infty}\int_C f(x)e^{-i\omega x}dx = 0 \tag{15}$$

and a sequence of functions $f_k \subset L^2[0,1]$ is said to weakly converge to f, denoted $f_k \rightharpoonup f$, if

$$\lim_{k\to\infty}\int_0^1 f_k(\tau)g(\tau)d\tau = \int_0^1 f(\tau)g(\tau)d\tau, \forall g \in L^2[0,1] \tag{16}$$

It is easily proven that h_1 and h_2 have uniform and weak limits, respectively written:

$$\lim_{\omega\to\infty}\int_{t_0}^t h_i\,d\tau = 0\ \forall i \tag{17a}$$

$$h_i\int_{t_0}^t h_j\,d\tau \rightharpoonup \lambda_{i,j} \tag{17b}$$

where $\rightharpoonup$ means "weak limit" (Scheinker and Krstić, 2017), and

$$\sqrt{\alpha}\omega cos(\omega t)\int_{t_0}^t \sqrt{\alpha}\omega cos(\omega\tau)\,d\tau \rightharpoonup \lambda_{1,1} = 0 \tag{18a}$$

$$\sqrt{\alpha}\omega cos(\omega t)\int_{t_0}^t -\sqrt{\alpha}sin(\omega\tau)\,d\tau \rightharpoonup \lambda_{1,2} = \frac{\alpha}{2} \tag{18b}$$

$$-\sqrt{\alpha}sin(\omega t)\int_{t_0}^t \sqrt{\alpha}\omega cos(\omega\tau)\,d\tau \rightharpoonup \lambda_{2,1} = -\frac{\alpha}{2} \tag{18c}$$

$$-\sqrt{\alpha}sin(\omega t)\int_{t_0}^t -\sqrt{\alpha}sin(\omega\tau)\,d\tau \rightharpoonup \lambda_{2,2} = 0 \tag{18d}$$

We now consider the integral by parts of the products b_i by h_i and obtain:

$$\begin{aligned}&\lim_{\omega\to\infty}\int_{t_0}^t b_i(\underline{x},\tau)h_i(\tau)d\tau\\ &= \lim_{\omega\to\infty}\left[b_i(\underline{x},\tau)|_{t_0}^t\int_{t_0}^t h_i(\tau)d\tau - \int_{t_0}^t\frac{db_i(\underline{x},\tau)}{d\tau}\int_{t_0}^t h_i(r)dr\,d\tau\right]\end{aligned} \tag{19}$$

The first term vanishes following (17a) and the second term can be expanded as:

$$\begin{aligned}&\lim_{\omega\to\infty}\int_{t_0}^t\frac{\partial b_i(\underline{x},\tau)}{\partial\tau}\int_{t_0}^t h_i(r)dr\,d\tau\\ &+\lim_{\omega\to\infty}\sum_{j=1}^2\int_{t_0}^t\frac{\partial b_i(\underline{x},\tau)}{\partial\underline{x}}b_j(\underline{x},\tau)h_j(\tau)\int_{t_0}^t h_i(r)dr\,d\tau\end{aligned} \tag{20a}$$

$$=\sum_{i\neq j}\int_{t_0}^t\frac{\partial b_i(\bar{\underline{x}},\tau)}{\partial\bar{\underline{x}}}b_j(\bar{\underline{x}},\tau)\lambda_{i,j}(t)d\tau \tag{20b}$$

where the overline $\bar{x}$ stands for averaged variables. The first term in (20a) vanishes due to (17a) and the second term yields (20b) in view of (18). Considering the dynamics of expression (20b), i.e., without the integral from t_0 to t, the average system or Lie-bracket system of (14) can be written:

$$\dot{\bar{e}} = f(\bar{\underline{x}}) + \frac{\partial b_1}{\partial\bar{\underline{x}}}b_2\lambda_{1,2} + \frac{\partial b_2}{\partial\bar{\underline{x}}}b_1\lambda_{2,1} \tag{21}$$

where $\bar{e}$ and $\bar{\underline{x}}$ stand for the average error and state trajectories, respectively. Combining (18) and (21) leads to:

$$\dot{\bar{e}} = f(\bar{\underline{x}}) - \frac{k\,\alpha}{2}g\,(\bar{\underline{x}})^T\,g\,(\bar{\underline{x}})\,\frac{\partial V\,(\bar{\underline{x}})}{\partial\bar{\underline{x}}} \tag{22}$$

We now adapt Theorem 4.4 from Scheinker and Krstić (2017) to the considered case study.

Theorem 1. *Consider the error system (9) and let there exist* $\eta \in \mathcal{K}_\infty$ *and* $\beta > 0$ *such that f and g satisfy the following bounds for all* $t \in \mathbb{R}^+$*:*

$$g\,(\bar{\underline{x}})^T\,g\,(\bar{\underline{x}}) \geq \beta,\ |f(\underline{x})| \leq \eta(\underline{x}) \tag{23}$$

Under the influence of the control law (11), with k and α *chosen such as:*

$$k\alpha > \frac{2}{\beta} \tag{24}$$

then the origin of (9) is $\left(\frac{1}{\omega}\right)$*-semiglobally practically uniformly ultimately bounded (SPUUB, including uniform stability).*

Proof From (12), the partial derivative with respect to the average state vector $\bar{\underline{x}}$ reads:

$$\frac{\partial V(\bar{\underline{x}})}{\partial \bar{\underline{x}}} = \eta\, X\, \frac{\bar{e}}{|\bar{e}|} + \eta\, |\bar{e}| \tag{25}$$

Defining a new Lyapunov function candidate

$$W(\bar{e}) = \frac{\bar{e}^2}{2} \tag{26}$$

we obtain its derivative

$$\dot{W}(\bar{e}) = \bar{e}\dot{\bar{e}} = \bar{e} f(\bar{\underline{x}}) - \bar{e}\frac{k\alpha}{2} g(\bar{\underline{x}})^T\, g(\bar{\underline{x}})\, \frac{\partial V(\bar{\underline{x}})}{\partial \bar{\underline{x}}} \tag{27}$$

Considering (23) and $|\bar{e} f| \leq |\bar{e}|\,\eta\, X$ in (27), we get

$$\dot{W}(\bar{e}) \leq |\bar{e}|\,\eta\, X - \frac{k\alpha}{2}\beta\left(\eta\, X\, |\bar{e}| + \eta\ |\bar{e}|^2\right) \tag{28}$$

and

$$\dot{W}(\bar{e}) \leq |\bar{e}|\,\eta\, X\left(1 - \frac{k\alpha}{2}\beta\left(1 + \frac{|\bar{e}|}{X}\right)\right) \leq |\bar{e}|\,\eta\, X\left(1 - \frac{k\alpha}{2}\beta\right) \tag{29}$$

To guarantee the negativeness of (29), (24) is imposed, ending the proof. The proposed extremum seeking loop (14) uniformly converges to the ethanol setpoint such that the origin of (9) is $\frac{1}{\omega}$-SPUAS (semi globally practically uniformly asymptotically stable; see (Moreau and Aeyels, 2000; Scheinker and Krstić, 2017) for further details). α and k can be used to tune the convergence rate. k can therefore be considered as a gain while α allows tuning both the periodic signal magnitude and the convergence rate.

3.4 Input saturation and switching dynamics

To guarantee the stabilization of (9), the input definition (11) assumes that u belongs to $\mathbb{R}$. However, the dilution rate is positive, which limits the input domain to $\mathbb{R}^+$ and invalidates the averaging results of section 3.3. This could lead to ethanol accumulation followed by loop destabilization. However, it is possible to show that a simple switching law triggered by an excess of ethanol accumulation can maintain closed-loop stability. We consider the following switching law where t_i and t_j represent two successive switching times ($i < j$) corresponding to the following situation:

$$e(t_i) < -\varepsilon \tag{30a}$$
$$e(t_j) > \delta \tag{30b}$$

where ε and δ are small positive constants triggering the input switches:

$$u(t) = \begin{cases} 0 & \forall e(t):\ e(t_i) \leq e(t) < e(t_j) \\ \alpha\sqrt{\omega}\, cos(\omega\, t) - k\,\sqrt{\omega}\, sin(\omega\, t)\, V(\underline{x}) & otherwise \end{cases} \tag{31}$$

We now resort to the stability theory of switched systems, using the common CLF (12). The following stability analysis constitutes a specific application of more general results which can be found, for instance, in (Chatterjee and Liberzon, 2006).

Consider the evolution of the CLF at successive switching instants t_i and t_j where $i < j$. It is possible to prove that despite the switching inputs, the CLF remains decreasing and reaches a specific bound. The difference of the corresponding CLF values reads:

$$V(t_j) - V(t_i) = \eta(X(t_j)\left|e(t_j)\right| - X(t_i)\left|e(t_i)\right|) \tag{32}$$

Under the specific switching time conditions defined in (30a) and (30b), (32) becomes:

$$V(t_j) - V(t_i) \leq \eta(X(t_j)\delta - X(t_i)\varepsilon) \tag{33}$$

and the stability condition requires to force the negativeness of the right-hand side of (33) $\forall(i,j)$ (Chatterjee and Liberzon, 2006).

Considering the approximation of the biomass ordinary differential equation (6a) as $\frac{X(t_j)-X(t_i)}{\Delta_{ij}} \approx F(\underline{x})X(t_i)$ where $F(\underline{x}) = k_{X1}r_1 + k_{X2}r_2 + k_{X3}r_3$ is the reactive contribution in (6a) and $\Delta_{ij} = t_j - t_i$, replacing $X(t_j)$ in (33), we get:

$$\frac{\varepsilon}{\delta} \leq F(\underline{x})\Delta_{ij} + 1 \tag{34}$$

Following the positiveness of $F(\underline{x})$, a simpler condition is

$$\frac{\varepsilon}{\delta} \leq 1 \tag{35}$$

This last condition states that despite the excursions above and below E_{ref} resulting from the saturation of u, the closed-loop stability is maintained.

4. NUMERICAL RESULTS

In the following, parameter tuning is provided, guided by the stability results of sections 3.3 and 3.4. A performance assessment of the proposed STAB-ESC with saturation is achieved on a lab-scale (10 L) yeast fed-batch culture simulation. For all simulations, state initial conditions are $X(t_0) = 0.4\ g/L$, $G(t_0) = 0\ g/L$ and $E(t_0) = 0\ g/L$ and the operating conditions are $V(t_0) = 5\ L$, $G_{in} = 350\ g/L$.

4.1 Parameter tuning

η is chosen as the upper bound of $f(\underline{x})$, as follows:

$$\eta = \sup_{\underline{x}}(k_{E2}r_1 + r_3) \tag{36}$$

Considering the definitions of r_1 and r_3 in (2) and (4), respectively, (36) is set to:

$$\eta = \mu_O\left(\frac{k_{E2}}{k_{os}} + \frac{1}{k_{oe}}\right) \tag{37}$$

The choice of β is made such that $g(\underline{x})^2 \geq \beta$. The order of magnitude of the product $k\alpha > \frac{2}{\beta}$ can therefore be approximated by $\frac{2}{(k_{E2}G_{in})^2} \approx 7\ 10^{-5}$. The selected value of β combined with the small order of magnitude of the dilution rate imposes $\alpha = 0.001$ and, in turn, $k = 0.070$. The values of the switching parameters ε and δ are respectively $0.01\ g/L$ and $0.02\ g/L$. All parameters are reported in Table 3.

Table 3. Tuning of the STAB-ESC strategy.

Parameter	*Value*	*Unit*
η	0.54	-
β	$7\ 10^{-5}$	
ω	100	h^{-1}
k	0.070	$h^{-1/2}$
α	0.001	$h^{-1/2}$
ε	0.010	gL^{-1}
δ	0.020	gL^{-1}

4.2 Performance analysis

Figure 1 shows the state trajectories and the ethanol tracking performance highlighted by successive setpoint E_{ref} changes, initially set at 0.3 g/L, increased at 0.5 g/L after 9 hours and decreased back at 0.3 g/L after 12 hours.

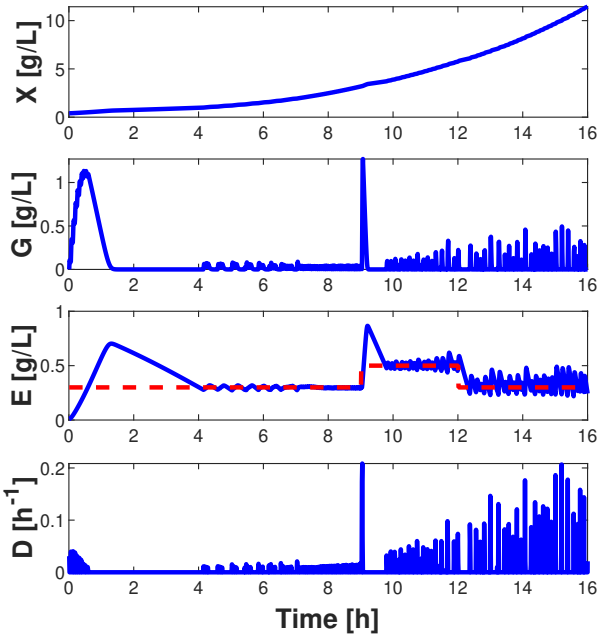

Fig. 1. Application of the STAB-ESC strategy to the yeast fed-batch culture model (6): state and input trajectories.

Despite a significant overshoot in the first 4 hours, the regulation is maintained until the first set-point change, where the system anew undergoes a smaller overshoot to set the regulation to $E_{ref} = 0.5\ g/L$. The closed-loop dynamic behavior following the decreasing step shows the effectiveness of the switching strategy. The corresponding root mean square error (RMSE) yields 0.13 g/L.

4.3 Robustness to noise

Measurement noise often limits the performance of most of the adaptive control techniques, including extremum seeking. Practically, measurement noise can be attenuated by low-pass filters in classical ES techniques, which however also tend to slow down the closed-loop dynamics. The partial derivatives $\frac{\partial b_i}{\partial \bar{x}}$ $(i = 1,2)$ of (21) contain the CLF which, if assumed noisy (i.e., V becomes $V + n(t)$ with n a Gaussian noise with zero mean), has an average value which is immune to noise. The derivative of the CLF with respect to the average variable $\bar{x}$, which is computed to obtain (22), is insensitive to noise and $\frac{\partial (V(\bar{x})+n)}{\partial \bar{x}} = \frac{\partial V(\bar{x})}{\partial \bar{x}}$. This means that despite the corrupted CLF measurement, on average, the system converges towards the extremum. It may be noticed that the switching dynamics do not alter the convergence robustness since condition (35) does not depend on n.

To confirm these statements, a Monte Carlo study is achieved, considering 30 runs with the same initial conditions from section 4.2. White noise with zero mean and a relative standard deviation of 5 % is applied to the biomass and ethanol measurements used in (12). Modern biomass and ethanol probe technologies allow better performance than the considered simulation conditions.

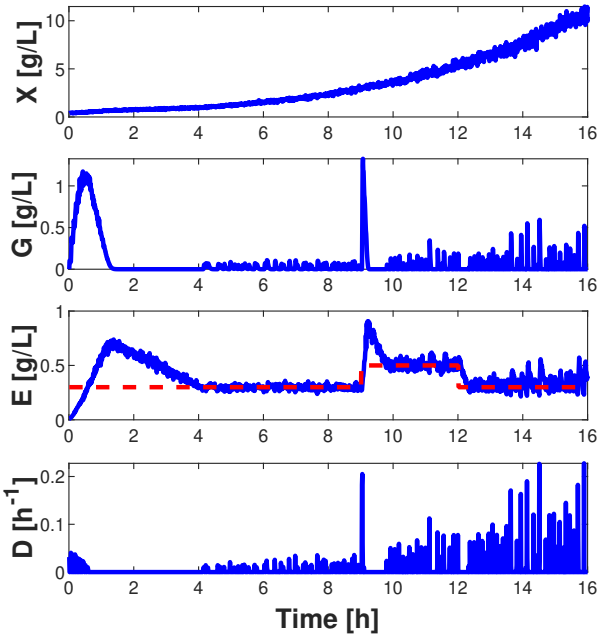

Fig. 2. Monte-Carlo analysis of the STAB-ESC application to the yeast fed-batch culture model (6): 30 runs with measurement noise (5% relative standard deviation): state and input trajectories.

Figure 2 shows that the noise may lead to slightly larger excursions of the ethanol signal (RMSE = 0.14 g/L) but the controller is still able to maintain stability with acceptable tracking dynamics. Significant variations of the final biomass concentration in 16 hours can be observed. Still, they are a direct consequence of the measurement noise which impacts the error variance without modifying the convergence properties.

5. CONCLUSION

The tracking of exponential feed rate trajectories remains challenging to optimize the productivity of yeast fed-batch cultures. The adaptive control framework remains essential since it allows for estimating the information on biomass growth from the biomass and ethanol measurements. Most of the existing adaptive control strategies are model-based and sensitive to measurement noise. In this study, a model-free stabilizing extremum-seeking strategy is proposed, constrained by input saturation leading to the consideration of switching closed-loop

dynamics. The method is computationally simple and shows promising results even in the presence of noise, as the same convergence properties are achieved. Further work entails experimental validations on a real industrial plant in a "good manufacturing practice" (GMP) environment.

REFERENCES

Akesson, M., Hagander, P., and Axelsson, J.P. (1999). A probing feeding strategy for escherichia coli cultures. *Biotechnology Techniques*, 13(8), 523–528.

Ariyur, K.B. and Krstic, M. (2003). *Real-time Optimization by Extremum-seeking Control*. John Wiley & Sons, INC, Wiley-Interscience edition.

Chatterjee, D. and Liberzon, D. (2006). Stability analysis of deterministic and stochastic switched systems via a comparison principle and multiple lyapunov functions. *SIAM Journal on Control and Optimization*, 45(1), 174–206.

Chichka, D.F., Speyer, J.L., Fanti, C., and Park, C.G. (2006). Peak-seeking control for drag reduction in formation flight. *Journal of guidance, control, and dynamics*, 29(5), 1221–1230.

Crabtree, H. (1929). Observations on the carbohydrate metabolism of tumors. *Biochemical Journal*, 23, 536–545.

Dewasme, L., Bogaerts, P., and Vande Wouwer, A. (2009). *Monitoring of bioprocesses: mechanistic and data-driven approaches*, 57–97. Studies in Computational Intelligence, (Computational Intelligent Techniques for Bioprocess Modelling, Supervision and Control, Maria do Carmo Nicoletti, Lakhmi C. Jain, eds.). Springer Verlag.

Dewasme, L., Coutinho, D., and Vande Wouwer, A. (2011a). Adaptive and robust linearizing control strategies for fed-batch cultures of microorganisms exhibiting overflow metabolism. *Lecture Notes in Electrical Engineering*, 89, 283–305.

Dewasme, L., Richelle, A., Dehottay, P., Georges, P., Remy, M., Bogaerts, P., and Vande Wouwer, A. (2010). Linear robust control of *S. cerevisiae* fed-batch cultures at different scales. *Biochemical Engineering Journal*, 53(1), 26–37.

Dewasme, L., Srinivasan, B., Perrier, M., and Vande Wouwer, A. (2011b). Extremum-seeking algorithm design for fed-batch cultures of microorganisms with overflow metabolism. *J. Process Control*, 21(7), 1092–1104.

Dewasme, L. and Vande Wouwer, A. (2020). Model-free extremum seeking control of bioprocesses: A review with a worked example. *Processes*, 8(10), 1209.

Dürr, H.B., Stanković, M.S., Ebenbauer, C., and Johansson, K.H. (2013). Lie bracket approximation of extremum seeking systems. *Automatica*, 49(6), 1538–1552.

Feudjio Letchindjio, C.G., Dewasme, L., and Vande Wouwer, A. (2021). An experimental application of extremum seeking control to cultures of the microalgae scenedesmus obliquus in a continuous photobioreactor. *International Journal of Adaptive Control and Signal Processing*, 35(7), 1285–1297.

Ghaffari, A., Krstić, M., and Seshagiri, S. (2014). Power optimization and control in wind energy conversion systems using extremum seeking. *IEEE Transactions on Control Systems Technology*, 22(5), 1684–1695.

Guay, M. and Dochain, D. (2017). A proportional-integral extremum-seeking controller design technique. *Automatica*, 77, 61–67.

Ibanez, F., Saa, P.A., Barzaga, L., Duarte-Mermoud, M.A., Fernandez-Fernandez, M., Agosin, E., and Perez-Correa, J. (2021). Robust control of fed-batch high-cell density cultures: a simulation-based assessment. *Computers and Chemical Engineering*, 155, 107545.

Khalil, H. (2002). *Nonlinear Systems*. Prentice-Hall, Upper Saddle River, NJ.

Koeln, J.P. and Alleyne, A.G. (2014). Optimal subcooling in vapor compression systems via extremum seeking control: Theory and experiments. *International journal of refrigeration*, 43, 14–25.

Marcos, N.I., Guay, M., and Dochain, D. (2004). Output feedback adaptive extremum seeking control for a continuous stirred tank bioreactor with monod's kinetics. *Journal of Process Control*, 14, 807–818.

Moase, W. and Manzie, C. (2012). Fast extremum-seeking for wiener-hammerstein plants. *Automatica*, 48, 2433–2443.

Monod, J. (1949). The growth of bacterial cultures. *Annual Review of Microbiology*, 3(1), 371–394.

Moreau, L. and Aeyels, D. (2000). Practical stability and stabilization. *IEEE Transactions on Automatic Control*, 45(8), 1554–1558.

Pimentel, G., Benavides, M., Dewasme, L., Coutinho, D., and Vande Wouwer, A. (2015). An observer-based robust control strategy for overflow metabolism cultures in fed-batch bioreactors. *IFAC-PapersOnLine*, 48(8), 1081–1086.

Poveda, J.I. and Krstic, M. (2021). Non-smooth extremum seeking control with user-prescribed fixed-time convergence. *IEEE Transactions on Automatic Control*, 66(12), 6156–6163.

Renard, F., Vande Wouwer, A., Valentinotti, S., and Dumur, D. (2006). A practical robust control scheme for yeast fed-batch cultures - an experimental validation. *Journal of Process Control*, 16, 855–864.

Scheinker, A. (2024). 100 years of extremum seeking: A survey. *Automatica*, 161, 111481.

Scheinker, A. and Krstić, M. (2017). *Model-free stabilization by extremum seeking*. Springer.

Silva, A.J.D., Rocha, C.K.d.S., and de Freitas, A.C. (2022). Standardization and key aspects of the development of whole yeast cell vaccines. *Pharmaceutics*, 14(12), 2792.

Sonnleitner, B. and Käppeli, O. (1986). Growth of *Saccharomyces cerevisiae* is controlled by its limited respiratory capacity : Formulation and verification of a hypothesis. *Biotechnol. Bioeng.*, 28, 927–937.

Sontag, E.D. (1989). A 'universal'construction of artstein's theorem on nonlinear stabilization. *Systems & control letters*, 13(2), 117–123.

Tan, Y., Moase, W., Manzie, C., Nesic, D., and Mareels, I. (2010). Extremum seeking from 1922 to 2010. In *Proceedings of the 29th Chinese Control Conference*, 14–26.

Titica, M., Dochain, D., and Guay, M. (2003). Adaptive extremum-seeking control of fed-batch bioreactors. *European Journal of Control*, 9(6), 618–631.

Valentinotti, S., Srinivasan, B., Holmberg, U., Bonvin, D., Cannizzaro, C., Rhiel, M., and von Stockar, U. (2003). Optimal operation of fed-batch fermentations via adaptive control of overflow metabolite. *Control engineering practice*, 11, 665–674.